Supplementary Materials and Methods

Animals

Wild-type C57BL/6N mice were purchased from Charles River Laboratories. CD6-deficient (*cd6*$^{-/-}$) mice were generated in C57BL/6N background as reported elsewhere [1]. NSG (NOD *scid* gamma) mice were originally purchased from the Jackson Laboratory (Bar Harbor, ME). Animals were kept under specific pathogen-free (SPF) conditions (with the exception of those for the EAE and CIA models, which were maintained under conventional housing conditions), and used at 7-8 weeks of age. The experimental protocols used were approved by the Ethics Committee for Animal Research of the University of Barcelona and all efforts were made to minimize animal suffering.

In vivo tumor growth assays

Assessment of syngeneic B16.F0 tumor cell growth was performed as reported elsewhere [2]. Briefly, B16.F0 tumor cells (5×10^4) were injected *s.c.* on the mid-dorsum of *cd6*$^{-/-}$ and WT (*cd6*$^{+/+}$) mice with a 23-gauge needle. For xenograft tumor growth, human melanoma A375 cells (1×10^6), kindly provided by Dr. Anna Macià (Institut de Recerca Biomèdica de Lleida, Spain), were injected *s.c.* in NSG mice and randomly assigned to treatment groups. Treatments were started two days after tumor challenged and continued for 3 weeks. Tumors were measured every other day with a Vernier caliper, and their diameter (Ø) or area measured in mm. At the end of the follow-up period tumors were excised and weighed (gr).

Liver Melanoma Metastasis assays

Liver metastasis formation was studied as previously described, with minor modifications [3]. Briefly, C57BL/6J mice receiving different *i.v.* AAV-smCD6 or AAV-Luc *v.g.*/mouse doses were challenged 2 weeks later with intrasplenic injection of B16.F0 cells (2.5×10^5). The number of liver metastasis, as well as liver and spleen weight were determined 3 weeks after challenge.

Statistical analyses

Results are given as mean ± SEM. Statistical analysis and data representation were performed with GraphPad Prism 6 Software. Statistical significance was set at $p \leq 0.05$.

Experimental autoimmune encephalomyelitis (EAE) model

Induction of EAE was performed as previously reported [4]. Briefly, female C57BL/6 mice (8–10 week old) were administered once *s.c.* with 0.25 µg/µL MOG35-55 (ref. EPK1, ESPIKEM) peptide in a final volume of 200 µL emulsified in CFA. At the time of immunization and 48 h later, 200 ng of *Bordetella pertusis* toxin (Sigma Aldrich) was injected *i.p.*. Clinical score was determined daily for 30 days and it represents the average value for each mice, where 0 = no disease; 0.5 = partially motionless tail; 1 = motionless tail; 2 = ataxia; 3 = loss of mobility in one limb; 4 = loss of mobility in back limbs; 5 = moribund; 6 = death.

Collagen-Induced Arthritis (CIA) model

Following a previously reported procedure [5], chicken collagen type II (CII; Chondrex) was dissolved at a concentration of 2 mg/mL in 50 mM acetic acid and emulsified with CFA containing 4 mg/mL of *Mycobacterium tuberculosis* (Chondrex). For the induction of CIA, male mice 8-12 weeks old were immunized once with 150 µg chicken CII in a final volume of 150 µL. The clinical score was assessed weekly with the following graded scale: 0 = no inflammation; 1 = detectable local swelling/erythema; 2 = swelling in >1 joint plus pronounced inflammation; 3 = swelling of the entire paw and/or ankylosis. Each paw was graded and scores added up (maximum score per mouse = 12).

Supplementary References

1. Orta-Mascaró M, Consuegra-Fernández M, Carreras E, Roncagalli R, Carreras-Sureda A, Alvarez P, Girard L, Simões I, Martínez-Florensa M, Aranda F, Merino R, Martínez V-GG, Vicente R, Merino J, Sarukhan A, Malissen M, Malissen B, Lozano F. CD6 modulates thymocyte selection and peripheral T cell homeostasis. J Exp Med 2016; 213: 1387-97.
2. Simões IT, Aranda F, Carreras E, Velasco-de Andrés M, Casadó-Llombart S, Martinez VG, Lozano F. Immunomodulatory effects of soluble CD5 on experimental tumor models. Oncotarget 2017; 8: 108156-69.
3. Long L, Rubin R, Brodt P. Enhanced invasion and liver colonization by lung carcinoma cells overexpressing the type 1 insulin-like growth factor receptor. Exp Cell Res 1998; 238: 116–21.

4. Vasquez M, Consuegra-Fernández M, Aranda F, Jimenez A, Tenesaca S, Fernandez-Sendin M, Gomar C, Ardaiz N, Di Trani CA, Casares N, Lasarte JJ, Lozano F, Berraondo P. Treatment of Experimental Autoimmune Encephalomyelitis by Sustained Delivery of Low-Dose IFN-α. J Immunol 2019; 203: 696–704.

5. Postigo J, Genre F, Iglesias M, Fernández-Rey M, Buelta L, Carlos Rodríguez-Rey J, Merino J, Merino R. Exacerbation of type II collagen-induced arthritis in apolipoprotein E-deficient mice in association with the expansion of Th1 and Th17 cells. Arthritis Rheum 2011; 63: 971–80.

Supplementary Figures

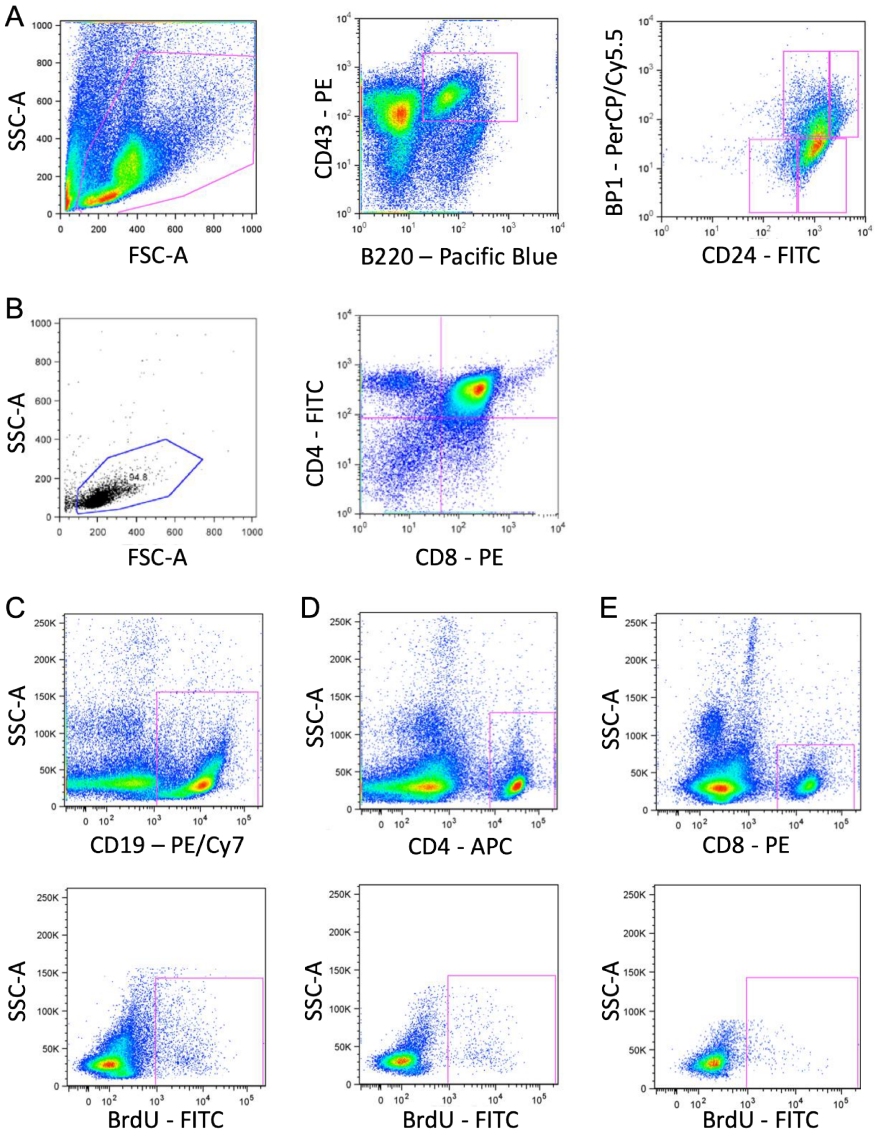

Fig. S1. Dot plots showing the gating strategy used in the analysis of lymphocyte subpopulations from primary and secondary mouse lymphoid organs. A) Gating strategy followed in the identification of bone marrow Pre-Pro B ($CD24^{low}BP1^{-}$), early Pro B ($CD24^{+}BP1^{-}$), late Pro B ($CD24^{+}BP1^{+}$) and Pre B ($CD24^{high}BP1^{+}$) cells. **B)** Gating

strategy followed in the identification of DN ($CD4^-CD8^-$), DP ($CD4^+CD8^+$), CD4SP ($CD4^+CD8^-$) and CD8SP ($CD4^-CD8^+$) thymocytes. **C-E)** Gating strategy followed in the identification of spleen $BrdU^+$ B ($CD19^+$) (**C**), Th ($CD4^+$) (**D**), and Tc ($CD8^+$) (**E**) cells.

Simões IT, *et al. J Immunother Cancer* 2020; 8:e000172. doi: 10.1136/jitc-2019-000172

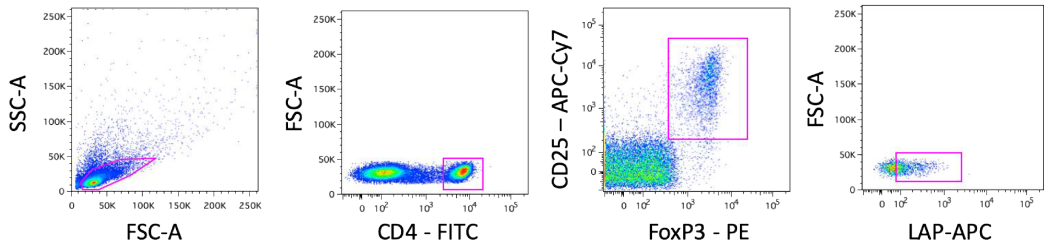

Fig. S2. Dot plots showing the gating strategy used in the analysis of functional Tregs. Gating strategy followed in the identification of spleen LAP^+ Treg ($CD25^+FoxP3^+/ CD4^+$) cells.

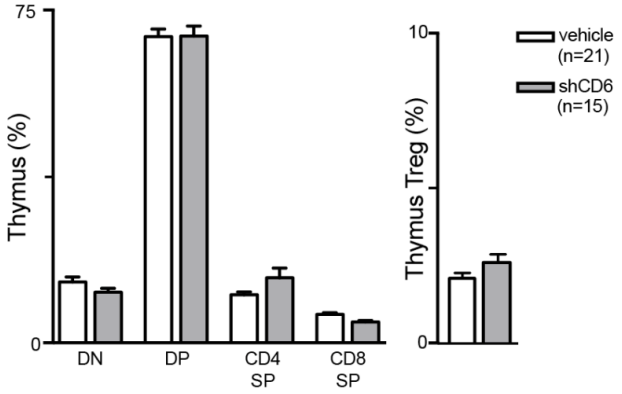

Fig. S3. Immunophenotypical analysis of thymus populations from WT mice treated with exogenous shCD6. Percentage of thymus DN, DP, $CD4^+$SP, $CD8^+$SP (**left**), and $CD25^+FoxP3^+$ in $CD4^+$T cells (Treg) (**right**) from C57BL/6N mice treated every 48 h for 14 days with 1.25 mg/kg of shCD6 or vehicle (PBS 10 % glycerol). Two-tailed Student's t-test was applied.

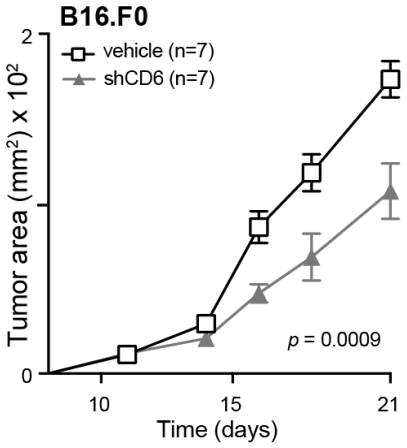

Fig. S4. Growth curves of *s.c.* implanted syngeneic melanoma cells into WT mice therapeutically infused with shCD6 protein. B16.F0 (5 x 10^4) cells were injected *s.c.* into WT mice and then shCD6 (1.25 mg/Kg) or vehicle (PBS 10% glycerol) were therapeutically administered every 48 h starting when tumor size was approx. 5-9 mm^2 (~day 9 post implantation). Tumor growth (area in mm^2) was monitored until sacrifice. Data are presented as mean ± SEM and two-way ANOVA test was used for statistical analysis.

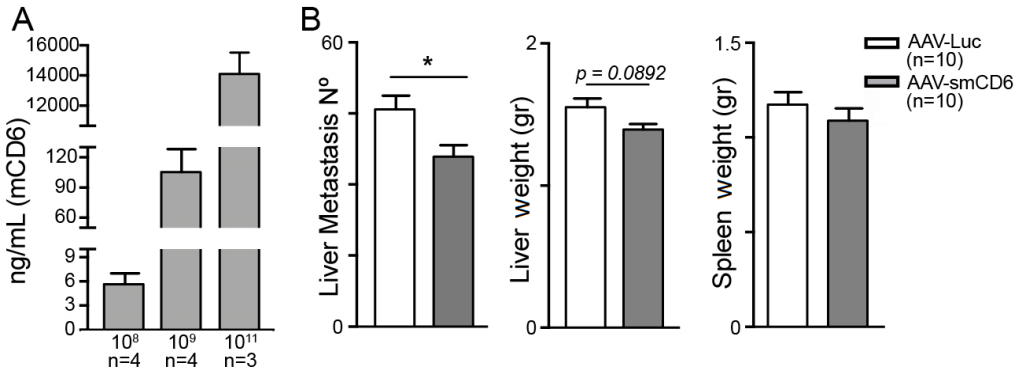

Fig. S5. Dose-course and metastatization assays in WT mice transduced with AAV-smCD6. A) C57BL/6J mice receiving different *i.v.* AAV-smCD6 *v.g.*/mouse doses (10^8, 10^9, and 10^{11}) were bled 2 weeks later for plasma smCD6 levels determination by ELISA. Data are expressed as mean ± SEM. **B)** C57BL/6J mice (n = 10/group) transduced *i.v.* with 10^{11} AAV-smCD6 or AAV-Luc *v.g.*/mouse were challenged 2 weeks later with B16.F0 (2.5×10^5) cells injected in the spleen. The number of liver metastasis and liver weight (gr) 3 weeks after challenge is represented. Spleen weight (primary tumor) is also represented. Data represent cumulative results from two independent experiments expressed as mean ± SEM. * $p < 0.05$; two-tailed Student's t-test.

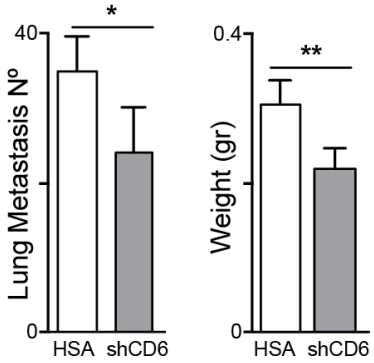

Fig. S6. Metastatization assays in WT mice treated with shCD6 protein. WT C57BL/6J mice were *i.p.* infused with 1.25 mg/kg of shCD6 or HSA 1 h before and after *i.v.* (tail vein) challenge with 2 x 10^5 B16.F0 cells (in 200 μL) previously incubated for 15 min with saturating amounts of shCD6 (25 μg/1x10^6 cells) or HSA. Number of lung metastasis (**left**) and lung weight (**right**) was determined 3 weeks after challenge. Data are expressed as mean ± SEM. * $p < 0.05$; ** $p < 0.01$; two-tailed Student's t-test.

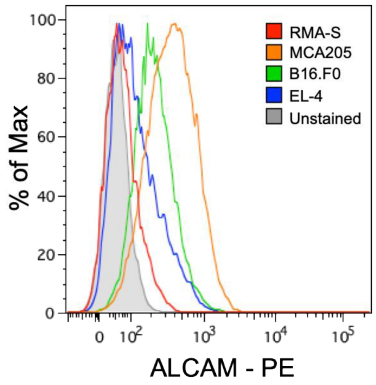

Fig. S7. Surface ALCAM/CD166 expression in different mouse tumor cell lines. FACS analysis of RMA-S, MCA205, B16.F0, and EL-4 tumor cell lines stained for surface ALCAM expression.

Simões IT, *et al. J Immunother Cancer* 2020; 8:e000172. doi: 10.1136/jitc-2019-000172

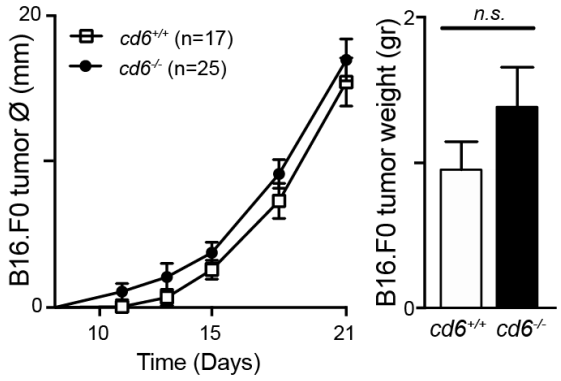

Fig. S8. Tumor growth in *cd*6-deficient mice. B16.F0 (5 x 10^4) cells were injected *s.c.* into WT ($cd6^{+/+}$) and *cd*6-deficient mice ($cd6^{-/-}$). Tumor growth (Ø, diameter in mm) and weight (gr) were measured every other day (**left**) and at the time of sacrifice (**right**), respectively. Cumulative data from two different experiments are represented as mean ± SEM. Two-way ANOVA and Mann Whitney tests were used for statistical analysis of tumor growth and weight, respectively.

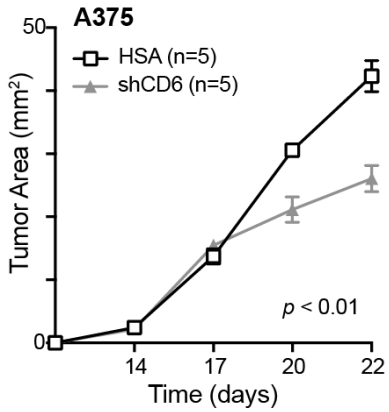

Fig. S9. Xenograft tumor growth in NSG mice. A375 cells (1 x 10^6) were injected *s.c.* into NSG mice, and tumor growth was measured every other day (area in mm). HSA or shCD6 (100 µg/mouse) were administered *i.p.* (200 µL/mouse) every other day starting at day 2 after tumor challenge and continued for 3 weeks. Two-way ANOVA and Mann Whitney tests were used for statistical analysis of tumor growth. The results are represented as mean ± SEM.

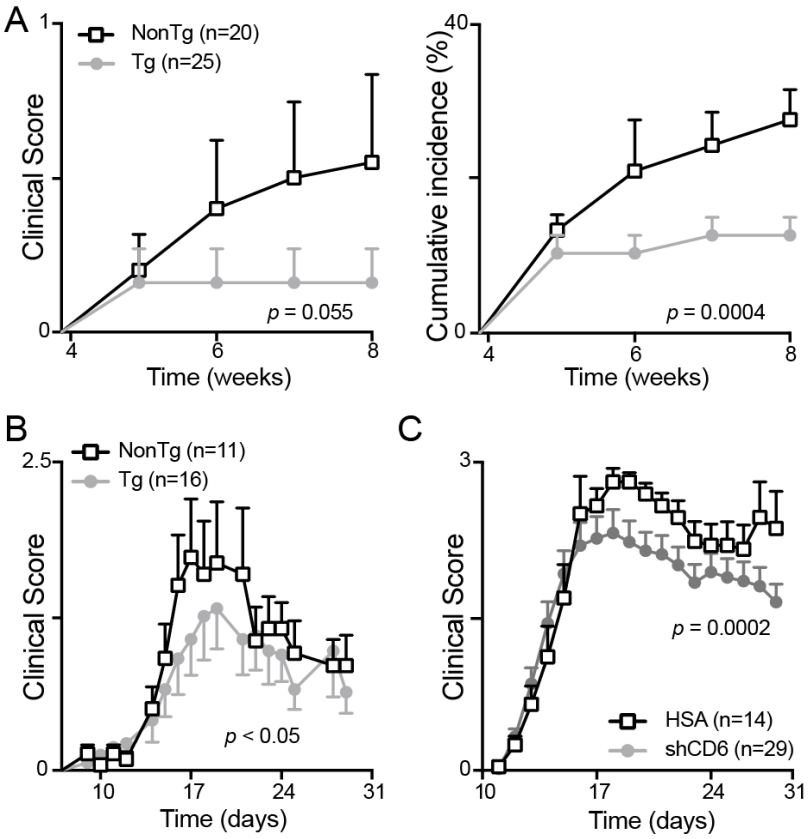

141

142 **Fig. S10. Attenuated autoimmune responses in shCD6LckEμTg and shCD6-treated**
143 **WT mice. A)** Weekly clinical scores (**left**) and cumulative incidence percentage (**right**)
144 in 7–8 week old male shCD6EμLckTg and NonTg mice subjected to CIA. **B)** Clinical
145 scores of 8–10 week old female shCD6EμLckTg and NonTg mice subjected to EAE.
146 Graph shows cumulative data from two independent experiments. **C)** Clinical scores of 8-
147 week-old WT female mice subjected to EAE and treated *i.p.* with 1.25 mg/kg shCD6 or
148 HSA (in PBS 10% glycerol) every 48 h, starting from day 0. Cumulative data from two
149 independent experiments are presented as mean ± SEM. Two-way tests were used for
150 statistical analysis.